

Graphical Abstract

Correlation-Weighted Communicability Curvature as a Structural Driver of Dengue Spread: A Bayesian Spatial Analysis of Recife (2015–2024)

Marcílio Ferreira dos Santos, Cleiton de Lima Ricardo, Andreza dos Santos Rodrigues de Melo

Highlights

Correlation-Weighted Communicability Curvature as a Structural Driver of Dengue Spread: A Bayesian Spatial Analysis of Recife (2015–2024)

Marcílio Ferreira dos Santos, Cleiton de Lima Ricardo, Andreza dos Santos Rodrigues de Melo

- We introduce correlation-weighted communicability curvature as a structural metric to explain spatiotemporal dengue patterns in dense urban environments.
- Curvature substantially reduces the spatially structured component in the BYM2-INLA model, capturing variability usually attributed to geographic adjacency.
- Annual shifts in mean curvature reveal changes in the underlying transmission architecture, with epidemic years showing more negative and structurally integrated networks.
- NDWI shows a significant effect, though its interpretation requires caution due to noise introduced by persistent cloud cover in tropical regions.
- Results highlight the value of integrating urban networks, spectral graph metrics, and hierarchical Bayesian modeling for high-resolution epidemiological surveillance.

Correlation-Weighted Communicability Curvature as a Structural Driver of Dengue Spread: A Bayesian Spatial Analysis of Recife (2015–2024)

Marcílio Ferreira dos Santos^{a,b}, Cleiton de Lima Ricardo^{b,c}, Andreza dos Santos Rodrigues de Melo^{a,b}

^aNúcleo de Formação de Docentes, Universidade Federal de Pernambuco (UFPE), , Caruaru, , PE, Brazil

^bNúcleo Interdisciplinar de Ciências Exatas e da Natureza (NICEN), Universidade Federal de Pernambuco (UFPE), , Caruaru, , PE, Brazil

^cDepartamento de Engenharia Cartográfica, Universidade Federal de Pernambuco (UFPE), , Recife, , PE, Brazil

Abstract

We investigate whether the structural connectivity of urban road networks helps explain dengue incidence in Recife, Brazil (2015–2024). For each neighborhood, we compute the average *communicability curvature*, a graph-theoretic measure capturing the ability of a locality to influence others through multiple network paths. We integrate this metric into Negative Binomial models, fixed-effects regressions, SAR/SAC spatial models, and a hierarchical INLA/BYM2 specification. Across all frameworks, curvature is the strongest and most stable predictor of dengue risk. In the BYM2 model, the structured spatial component collapses ($\phi \approx 0$), indicating that functional network connectivity explains nearly all spatial dependence typically attributed to adjacency-based CAR terms. The results show that dengue spread in Recife is driven less by geographic contiguity and more by network-mediated structural flows.

Keywords: Dengue, Spatial Epidemiology, Correlation-Weighted Communicability Curvature, Network Science, Bayesian Hierarchical Models, INLA

1. Introduction

Dengue remains one of the most significant vector-borne diseases worldwide, with estimates indicating nearly 390 million infections annually and recurrent outbreaks across tropical and subtropical regions. Its primary vector, the *Aedes aegypti* mosquito, exhibits complex ecological and epidemiological dynamics that continue to challenge surveillance and control programs [1, 2, 3].. Despite the extensive body of knowledge on vector biology, uncertainties persist regarding how human cases cluster in time and space, and how these clusters can be translated into transmission trajectories that are informative for public health decision-making.

Traditional epidemiological models, such as compartmental frameworks (SIR and related variants), cap-

ture aggregated trends but often overlook the fine-scale spatiotemporal dynamics underlying vector–host interactions [4, 5, 6]. Graph- and topology-based approaches offer a complementary perspective by explicitly representing the potential connections among cases, enabling the investigation of transmission chains, local clusters, and structural properties of outbreaks. Although such approaches have gained traction within network epidemiology [7, 8], they remain underexplored in the context of dengue transmission in urban environments.

The construction of realistic topological models for dengue depends on defining biologically plausible temporal and spatial windows. Empirical studies provide key parameters: the average flight range of *Aedes aegypti* is approximately 105 m, rarely exceeding 200 m [11], while the extrinsic incubation period of the dengue virus within the mosquito varies between 6 and 14 days [12]. Incorporating these parameters enables the development of models that approximate either (i) transmission chains, in which one case leads to another through the vector–host cycle, or (ii) co-infection clusters, in which multiple cases share a common infection source within a defined spatiotemporal window [9, 10].

In this study, we introduce a modeling framework grounded in street-level time series, taking advantage

*Corresponding author.

Email addresses: marcilio.santos@ufpe.br (Marcílio Ferreira dos Santos), cleiton.lricardo@ufpe.br (Cleiton de Lima Ricardo), andreza.rodrigues@ufpe.br (Andreza dos Santos Rodrigues de Melo)

URL: <https://orcid.org/0000-0001-8724-0899> (Marcílio Ferreira dos Santos), <https://orcid.org/0000-0002-7114-1201> (Cleiton de Lima Ricardo), <https://orcid.org/0000-0002-5153-6548> (Andreza dos Santos Rodrigues de Melo)

of the fact that public health records in Recife include the precise location of each reported case. This enables us to relate and compare temporal patterns across streets and to identify statistical zones of influence emerging from their time series. We employ a contemporary network metric — communicability curvature [7, 15]—which quantifies the importance of a given edge to the integrity of the graph’s connected component. The rationale behind this analysis is to identify influential “arteries,” or critical corridors, that play a disproportionately important role in the topological structure of dengue transmission. The removal or disruption of such edges would likely hinder the maintenance of dengue incidence, providing a highly localized and cost-effective strategy for outbreak mitigation.

2. Graph-Based Modelling of Transmission Topology

In this section, we formalize the graph-based modelling framework adopted to represent the spatiotemporal dynamics of dengue cases. Graphs offer a versatile structure because they encode both the geographic distribution of cases and the temporal relationships underlying dengue transmission. The construction follows established principles in the network epidemiology literature and serves as the structural basis for all analyses presented in this article.

2.1. Local Time Series Model

This model is closely aligned with recent formulations used in spatial epidemiology and the study of complex systems [13, 8]. Each vertex corresponds to a georeferenced point representing the street where cases were recorded, and each vertex is associated with a local incidence time series. Edges are established between vertices whose temporal similarity—here measured by the correlation between their respective series—exceeds a predefined threshold, indicating epidemiological synchrony between distinct locations.

To illustrate the resulting structural connectivity, Figure 1 shows the functional street-level graph superimposed on the geographic map of Recife. This visualization highlights the major channels of structural flow induced by correlated dengue activity and provides a geometric understanding of the network used throughout the study.

The epidemiological interpretation is direct: highly correlated time series may reflect

- (i) exposure to a common source of infectious mosquitoes, or

- (ii) localized diffusion processes mediated by the vector over time.

Incorporating this statistical layer allows the identification of spatiotemporal clusters with greater robustness than purely spatial approaches. Analogous correlation-based graph models were widely explored during the COVID-19 pandemic, where they were used to quantify systemic fragility and epidemic risk [14, 24, 5].

Formally, this construction yields a graph $G = (V, A)$, where the vertex set V represents streets and the edge set A connects pairs of temporally synchronized time series. Such a structure enables the application of topological and spectral metrics—including discrete curvature measures—to characterize structural bottlenecks and diffusive patterns in the network.

To ensure biological plausibility, an additional spatial pruning criterion is applied: only pairs of points separated by less than 600 m are connected. This threshold represents approximately three times the average flight range of *Aedes aegypti* [11], accounting for geocoding uncertainty and for the approximation inherent in using street centroids [25, 6].

Among the candidate models evaluated, we chose to develop the local time series model in depth due to its conceptual alignment with established methodologies, its ability to capture fine-scale epidemiological synchrony, and its direct applicability to real municipal surveillance data.

3. Theoretical and Empirical Results

In this section, we present the mathematical foundations that justify the use of communicability curvature as a diffusion-sensitive metric in epidemiological graphs, together with an empirical analysis based on real dengue data from the Metropolitan Region of Recife. The aim is to demonstrate, in an integrated manner, both the formal consistency of the approach and its practical utility for monitoring and interpreting transmission dynamics.

The analysis of mean curvature across neighborhoods reveals distinct spatial patterns in the structure of dengue dissemination over the historical series. Here, curvature is interpreted as an indicator of the structural coherence of the transmission graph: more negative values correspond to highly integrated networks that favor propagation, whereas higher values indicate spatial fragmentation and reduced connectivity among nodes.

In 2015, we observe a predominance of negative or near-zero curvature across much of the territory. This behavior is characteristic of a highly connected graph in

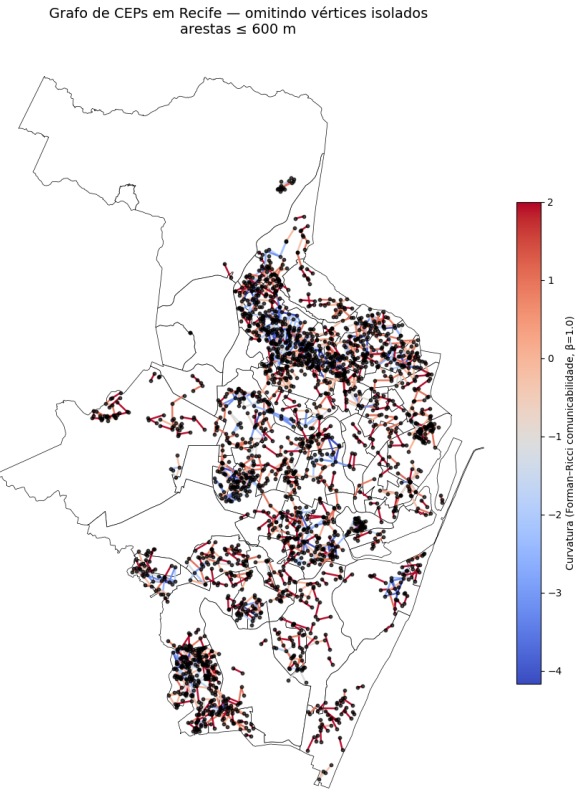


Figure 1: Street-level functional connectivity graph for Recife. Nodes represent geocoded dengue case locations, and edges denote correlated local incidence time series. The graph is superimposed on the geographic map to reveal the underlying transmission topology, highlighting structural pathways and spatial constraints that shape diffusive spread.

which multiple epidemiological pathways exist among different regions of the city. Such structure facilitates rapid viral diffusion, consistent with the fact that 2015 was one of the most critical years of the decade, marked by simultaneous and widely distributed outbreaks. The spatial pattern suggests that the virus encountered few territorial barriers, forming a functionally integrated urban mesh conducive to widespread transmission.

In 2019, the spatial pattern changes significantly: curvature values become higher, indicating a reduction in structural connectivity. This behavior aligns with the sharp decline in dengue cases recorded during that period. The increase in curvature suggests that transmission became more localized, with contagion chains restricted to specific subsets of neighborhoods. Structurally, 2019 represents a scenario of greater segmentation and increased spatial resistance to viral circulation.

In 2024, we observe a partial reconstitution of epidemiological connectivity. Although the number of cases rises again, the spatial pattern does not reproduce

the diffuse collapse seen in 2015. Curvature values exhibit greater heterogeneity, combining regions of positive curvature with localized pockets of negative curvature. This arrangement indicates a moderate diffusion capacity, concentrated in specific urban clusters. The network recovers some connectivity, yet remains less integrated than in 2015, resulting in substantial but more spatially delimited outbreaks.

Comparing these three years reveals a consistent pattern: (i) in 2015, the urban network exhibited high connectivity, favoring broad diffusion; (ii) in 2019, structural fragmentation drastically reduced the potential for transmission; and (iii) in 2024, the system assumes an intermediate configuration marked by localized outbreaks and moderate connectivity. These results demonstrate that spatial curvature captures the structural dynamics of epidemiological risk, distinguishing periods of heightened susceptibility to widespread dissemination from those in which transmission tends to remain confined.

Thus, the maps presented do not merely depict case intensity; they reveal how the spatial architecture of transmission reorganizes over time. Communicability curvature therefore emerges as a relevant complementary tool for geographically targeted epidemiological surveillance, enabling the anticipation of diffusion patterns and guiding more precise interventions.

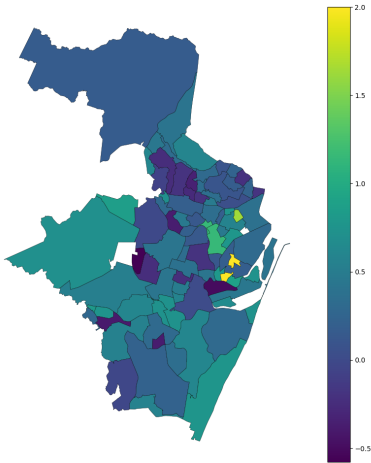


Figure 2: Mean communicability curvature by neighborhood in 2015.

3.1. Theoretical Results

The construction of the epidemiological graph allows the communicability $C_{ij}(\beta)$ to be interpreted as a measure of accessibility between vertices, incorporating all possible transmission routes weighted by the topological cost of each path [15, 7, 16, 17]. Before presenting the key results, we introduce the formal definition of communicability and the role of the parameter β , both essential for the subsequent epidemiological interpretation.

Communicability and Walks. Let $G = (V, E)$ be a simple, undirected, nonnegative graph with adjacency matrix $A = [A_{ij}]$. The *communicability* between two vertices i and j is defined as

$$C_{ij}(\beta) = (e^{\beta A})_{ij},$$

where the matrix exponential admits the classical expansion

$$e^{\beta A} = \sum_{k=0}^{\infty} \frac{\beta^k}{k!} A^k.$$

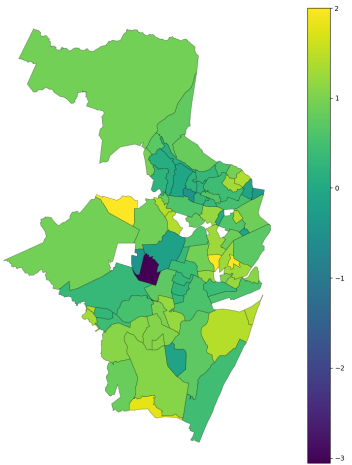


Figure 3: Mean communicability curvature by neighborhood in 2019.

Since $(A^k)_{ij}$ counts the number of walks of length k between i and j , communicability sums all possible routes, weighting longer paths by decaying factors $\beta^k/k!$. Thus, $C_{ij}(\beta)$ captures structural accessibility across multiple scales [7, 15, 29], from local neighborhoods to global connections.

The parameter $\beta > 0$ controls the relative contribution of paths of different lengths: for $0 < \beta \leq 1$, long paths still contribute, but with rapidly decreasing weight. Moreover,

$$\lim_{k \rightarrow \infty} \frac{\beta^k}{k!} = 0 \quad (\beta > 0),$$

since the superexponential growth of the factorial dominates any fixed power of β . Hence, very long walks have asymptotically negligible contribution, and the series is absolutely convergent.

Role of the Parameter β . The parameter $\beta > 0$ acts as a *scale controller* of diffusion:

- For small β , only short paths contribute significantly, emphasizing local relationships.
- For large β , long paths become relevant, revealing global connectivity.

The interpretation parallels statistical physics, in which $\beta = 1/T$ represents the inverse temperature: large β corresponds to stronger structural coupling and greater influence of distant routes.

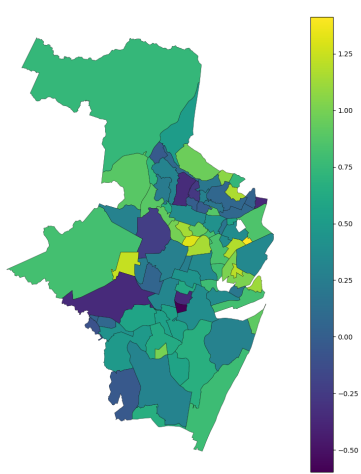


Figure 4: Mean communicability curvature by neighborhood in 2024.

With this foundation, we now present three results that justify communicability as a measure of epidemiological accessibility.

Proposition 1 (Monotonicity of Communicability). *Let $G = (V, E)$ be a simple nonnegative graph with adjacency matrix A . For any vertices $i, j \in V$ and parameters $\beta_1 < \beta_2$,*

$$C_{ij}(\beta_1) \leq C_{ij}(\beta_2).$$

Proof. From the series expansion,

$$C_{ij}(\beta) = \sum_{k=0}^{\infty} \frac{\beta^k}{k!} (A^k)_{ij},$$

all coefficients $\beta^k/k!$ are nonnegative and increase monotonically in β . Since $(A^k)_{ij} \geq 0$ for all k , it follows that $C_{ij}(\beta)$ increases monotonically in β . \square

Epidemiological Interpretation. The parameter β reflects the intensity of the diffusive process. During periods of high transmissibility or widespread outbreaks, long paths contribute more to propagation, increasing the functional connectivity of the system. An increase in β therefore corresponds to a regime in which the global structure of the network plays a stronger role in epidemic spread.

Theorem 1 (Communicability as a Diffusion Approximation). *Consider the linear process on G described*

by

$$\frac{dX(t)}{dt} = \beta A X(t), \quad X(0) = e_i.$$

Its solution is

$$X(t) = e^{\beta t A} e_i,$$

so the expected influence on vertex j at time t is proportional to the communicability $C_{ij}(\beta t)$.

Epidemiological Interpretation. The solution shows that $e^{\beta t A}$ acts as a propagation operator on the graph. Communicability thus emerges naturally as an approximation of linearized epidemic diffusion, linking network structure to potential transmission trajectories.

Proof. This follows directly from the standard solution of a linear differential equation via the matrix exponential. \square

Proposition 2 (Percolation Threshold Maximizes Mean Communicability). *Let G_τ be the graph obtained by thresholding correlations between local time series, and let $L(\tau)$ denote the size of the giant component of G_τ . Then there exists τ^* near the percolation threshold such that the mean communicability*

$$\bar{C}(\tau) = \frac{1}{|V|^2} \sum_{i,j \in V} C_{ij}(\beta)$$

is maximized at $\tau = \tau^$.*

Epidemiological Interpretation. Near the percolation threshold, the network transitions from a fragmented regime to one with large, yet not overly dense, connected components. In this critical region, the number of alternative paths and the structural reach between vertices are maximized, making communicability particularly sensitive to identifying diffusive bottlenecks and potential preferential transmission routes.

Lemma 1 (Spectral Representation of Communicability). *Let A_τ be the adjacency matrix of the thresholded graph G_τ . Then the mean communicability can be written as*

$$\bar{C}(\tau) = \frac{1}{|V|^2} \sum_{k=1}^n e^{\beta \lambda_k(\tau)},$$

where $\lambda_1(\tau) \geq \dots \geq \lambda_n(\tau)$ are the eigenvalues of A_τ .

Proof. From the spectral decomposition $A_\tau = Q_\tau \Lambda_\tau Q_\tau^\top$ and

$$e^{\beta A_\tau} = Q_\tau e^{\beta \Lambda_\tau} Q_\tau^\top,$$

the sum of entries of $e^{\beta A_\tau}$ depends only on the eigenvalues, since

$$\text{tr}(e^{\beta A_\tau}) = \sum_{k=1}^n e^{\beta \lambda_k(\tau)}.$$

Normalization by $|V|^2$ yields the desired expression. \square

Lemma 2 (Spectral Growth at the Percolation Threshold). *Let G_τ be a family of graphs obtained by thresholding correlations and let $L(\tau)$ denote the size of the giant component. Then the derivative*

$$\frac{d}{d\tau} \lambda_1(\tau)$$

is maximized near the percolation threshold.

Proof. Classical results in spectral percolation theory (Bollobás–Riordan, 2004; Krivelevich, 2013; Chung–Lu, 2006) show that for monotone edge-addition processes, the transition from subcritical to supercritical regimes coincides with the most abrupt change in $\lambda_1(\tau)$, corresponding to the sudden emergence of the giant component. \square

Lemma 3 (Path Diversity at the Critical Threshold). *For each $m \geq 1$, the total*

$$S_m(\tau) = \sum_{i,j \in V} (A_\tau^m)_{ij}$$

is maximized when G_τ lies near the percolation threshold.

Proof. The term $(A_\tau^m)_{ij}$ counts the number of walks of length m between i and j . Fragmented graphs yield few walks; overly dense graphs yield many redundant walks. Near the critical threshold, structural diversity is maximized (Newman, 2010). \square

Lemma 4 (Critical Behavior of the Matrix Exponential). *If $e^{\beta A_\tau} = \sum_{m=0}^{\infty} \frac{\beta^m}{m!} A_\tau^m$, then the sum*

$$T(\tau) = \sum_{i,j} (e^{\beta A_\tau})_{ij}$$

is maximized near the percolation threshold.

Proof. From the series expansion,

$$T(\tau) = \sum_{m=0}^{\infty} \frac{\beta^m}{m!} \sum_{i,j} (A_\tau^m)_{ij}.$$

By Lemma 3, each summand is maximized at the critical threshold. Since the coefficients $\beta^m/m!$ are positive, the full sum inherits this maximum. \square

Proposition 3 (Percolation Threshold Maximizes Mean Communicability). *Let G_τ be the thresholded correlation graph and $L(\tau)$ the size of its giant component. Then there exists τ^* near the percolation threshold such that*

$$\bar{C}(\tau) = \frac{1}{|V|^2} \sum_{i,j} C_{ij}(\beta)$$

is maximized at $\tau = \tau^$.*

Proof. By Lemma 1,

$$\bar{C}(\tau) = \frac{1}{|V|^2} \sum_{k=1}^n e^{\beta \lambda_k(\tau)}.$$

By Lemma 2, $\lambda_1(\tau)$ is maximized at the critical threshold. By Lemmas 3 and 4, walk diversity and the matrix exponential also peak in that region. Thus the total sum of entries of $e^{\beta A_\tau}$, and hence $\bar{C}(\tau)$, is maximized near the percolation threshold. \square

3.2. Correlation-Weighted Communicability Curvature

Communicability curvature identifies structural bottlenecks by quantifying the importance of each edge to the global connectivity of the graph. However, its classical formulation depends solely on the topological structure and does not incorporate dynamic information from the local time series that reflect the evolution of the epidemic.

To integrate these two dimensions—structure and dynamics—we propose a modified metric that combines communicability with temporal correlation between vertices. Let $C_{ij}(\beta)$ denote the communicability between vertices i and j ,

$$C_{ij}(\beta) = (e^{\beta A})_{ij},$$

and let $w_{ij} \in [0, 1]$ be the weight associated with the correlation between the local incidence time series at i and j .

Definition 1 (Correlation-Weighted Communicability Curvature). *We define the correlation-weighted communicability curvature as*

$$\kappa_{ij} = C_{ij}(\beta) w_{ij}.$$

The metric κ_{ij} highlights edges that simultaneously exhibit (i) high structural importance—as measured by communicability; and (ii) strong epidemiological synchrony—as captured by the correlation weights w_{ij} .

Unlike classical curvature, which relies solely on graph topology, the proposed metric incorporates dynamic information directly tied to transmission processes. In urban epidemiological settings, κ_{ij} identifies

connections that not only support the diffusive structure of the graph but also display strong temporal association, representing potential preferential corridors of dengue dissemination.

Thus, κ_{ij} is conceptually related to notions such as effective transmissibility and local risk flow, providing a rigorous bridge between the topology of complex networks and spatiotemporal incidence patterns.

4. Empirical Results

In this section, we evaluate whether the mean communicability curvature of road-network graphs is a robust determinant of annual dengue incidence in the Metropolitan Region of Recife. Several models were estimated with complementary objectives:

1. to establish an epidemiologically adequate baseline model,
2. to control for unobserved heterogeneity across neighborhoods,
3. to capture residual spatial dependence,
4. to validate robustness via modern Bayesian modeling.

Only the essential results are summarized below.

4.1. Negative Binomial Model

The Negative Binomial model showed excellent fit and confirmed that **mean curvature is a strong negative predictor of dengue incidence**. The main findings are:

1. curvature coefficient: $\beta = -1.07$ ($p < 0.001$);
2. effect size: a 1-unit increase in curvature reduces expected incidence by approximately 65%;
3. the effect remains stable after controlling for environmental and sociodemographic variables.

The Negative Binomial model serves as the “baseline model,” demonstrating that the relationship between curvature and epidemiological risk is structural and does not depend on the inclusion of explicit spatial terms.

4.2. Spatial and Temporal Fixed Effects

We estimated a linear model with fixed effects for neighborhood and year, absorbing spatial heterogeneity and seasonal epidemic cycles.

Results show that:

1. curvature remains statistically significant ($p < 0.01$);
2. the model explains approximately $R^2 \approx 0.57$;
3. fixed effects capture persistent differences between neighborhoods and inter-annual epidemic cycles.

Even after controlling for time-invariant neighborhood characteristics, the effect of road-network structure remains robust.

As shown in [20], hierarchical Bayesian models can identify, with high accuracy, the neighborhoods that consistently lead dengue incidence over the years. Incorporating correlation-weighted curvature deepens this ability by capturing structural properties of the urban network that are not reflected in traditional socioenvironmental covariates. Thus, including this metric yields more stable predictions, reduced spatial uncertainty, and more informative risk maps, particularly valuable for targeted public-health interventions and resource allocation.

4.3. Classical Spatial Models (SAR and SAC)

Traditional spatial models—the *Spatial Autoregressive Model* (SAR) and the *Spatial Autoregressive Combined* (SAC)—were fitted as an intermediate step to assess residual spatial dependence prior to hierarchical Bayesian modeling [29, 18]. Both models used the Queen contiguity matrix, despite the structural fragmentation of the mesh (33 disconnected components), a typical feature of cities with heterogeneous morphology [18].

Despite this topological limitation, the models produced stable estimates consistent with the remaining results. The SAR model exhibited $\text{Pseudo-}R^2 = 0.424$, while the SAC model yielded a similar value (0.421). These values indicate that a substantial portion of spatial variability is captured by the covariates, although enough residual autocorrelation remains to justify a hybrid spatial-random-effects approach (e.g., BYM2 or SPDE-INLA) [19].

Table 1: Comparison of main coefficients for the reduced SAR and SAC models.

Variable	SAR (coef.)	SAC (coef.)	Significance
Curvature	−47.32	−47.11	***
Year	−11.67	−11.85	***
Precipitation (lag 3)	+0.376	+0.386	***
Seasonality	+21.49	+21.25	***
Population density	+0.0061	+0.0053	***
Inequality (richest share)	−33.40	−30.52	***
Slum proportion	−32.09	−25.59	**
<i>Model diagnostics</i>			
Pseudo- R^2	0.424	0.421	—
Spatial lag Wy	−0.102 (n.s.)	+0.091 (n.s.)	—

Consistent findings across SAR and SAC

In both models:

1. the **correlation-weighted curvature** remained a highly significant negative coefficient (SAR: −47.3; SAC: −47.1; $p < 0.001$), reinforcing its interpretation as a structural determinant of dengue diffusion;
2. the temporal effect was strongly decreasing (approx. −11.7 cases/km² per year);
3. 3-month lagged precipitation maintained a stable positive effect (SAR: 0.376; SAC: 0.386);
4. rainy-season effects were consistently positive (\approx 21 cases/km²);
5. population density and inequality (richest income share) retained robust structural effects.

The spatial lag term Wy , however, was not statistically significant (SAR: $p = 0.20$; SAC: $p = 0.40$), suggesting that spatial dependence does not operate primarily through autocorrelation between adjacent areas, but rather through structural gradients in the urban environment—supporting the use of hierarchical models such as BYM2 [19, 32], which represent spatial smoothing more flexibly.

The results indicate that most spatial dependence is explained by urban, environmental, and structural covariates, whereas the autocorrelation traditionally represented by Wy is essentially null. This implies that dengue dynamics in Recife do not behave as a purely contagious process between adjacent areas, but rather as a phenomenon structured by urban and socioenvironmental gradients across the territory.

In this context, **correlation-weighted communicability curvature** emerges as a particularly expressive mechanism: by quantifying multiple and redundant

paths between locations, it captures *functional connectivity* that transcends mere geographic adjacency. The strong significance of curvature suggests that network-derived metrics reflect the spatial forces relevant to dengue propagation—possibly replacing or refining the role of classical spatial autocorrelation.

This evidence reinforces the natural transition to hierarchical Bayesian approaches (BYM2) and continuous spatial models (SPDE), which treat spatial dependence more flexibly and in closer agreement with the empirical pattern.

4.4. INLA/BYM2 Model: Latent Spatial Structure and Robustness

As the final stage of the empirical analysis, we estimated a hierarchical spatial model of the Besag–York–Mollié family in its BYM2 parametrization, using the Integrated Nested Laplace Approximation (INLA) [31, 19]. This model is widely employed in contemporary spatial epidemiology because it decomposes variability into a *structured* component (neighborhood-based) and an *unstructured* component, while providing accurate inference for the latent process via hyperparameters.

The objectives of this subsection are:

- to confirm the robustness of effects estimated in the Negative Binomial, fixed-effects, and SAR/SAC models;
- to evaluate the behavior of mean communicability curvature in a state-of-the-art hierarchical spatial model;
- to characterize residual spatial structure through BYM2 hyperparameters.

Table 2: Fixed effects from the INLA/BYM2 model. Coefficients represent posterior means and 95% credible intervals.

Variable	Mean	SD	2.5%	Median	97.5%
<i>Structural and climatic covariates</i>					
Year (numeric)	-11.75	0.90	-13.52	-11.75	-9.98
Curvature	-46.41	3.99	-54.24	-46.41	-38.58
Mean annual precipitation	-0.02	0.01	-0.04	-0.02	-0.004
Precipitation (lag 3)	0.37	0.07	0.24	0.37	0.50
Rainy season indicator	21.58	3.32	15.08	21.58	28.09
<i>Socioeconomic covariates</i>					
Slum proportion (%)	-25.84	12.93	-51.19	-25.85	-0.48
Population density	0.0056	0.0004	0.0048	0.0056	0.0065
Richest income share (%)	-28.43	8.34	-44.79	-28.43	-12.06
Total population	-0.00044	0.00015	-0.00074	-0.00044	-0.00014

Table 3: BYM2 hyperparameters estimated using INLA.

Hyperparameter	Mean	SD	2.5%	Median	97.5%
Precision (Gaussian)	$1.39 \cdot 10^{-4}$	$5.77 \cdot 10^{-6}$	$1.28 \cdot 10^{-4}$	$1.39 \cdot 10^{-4}$	$1.51 \cdot 10^{-4}$
Precision (structured)	4.52	0.30	3.92	4.51	5.11
ϕ (structured share)	$5.41 \cdot 10^{-10}$	$1.16 \cdot 10^{-10}$	$3.02 \cdot 10^{-10}$	$5.48 \cdot 10^{-10}$	$7.26 \cdot 10^{-10}$

Fixed Effects

Table 2 presents the posterior summary of fixed effects. The coefficients show strong agreement with the classical models, reinforcing the stability of environmental, demographic, and structural predictors.

Notably, **communicability curvature** retains a highly significant and strongly negative coefficient (mean = -46.4), with a narrow credibility interval. Its magnitude surpasses all other covariates, confirming that the geometry of the urban network is a structural predictor of dengue diffusion.

Spatial Hyperparameters

Table 3 presents the hyperparameters of the spatial component. Two results are particularly important:

(i) ϕ is effectively zero.. The parameter ϕ measures the proportion of spatial variance explained by the structured CAR component. The estimate

$$\phi \approx 5 \times 10^{-10},$$

is essentially zero. In practical terms:

After including communicability curvature and the other covariates, no meaningful residual spatial dependence remains to be explained by Queen-type neighborhood adjacency.

This is a substantive finding: curvature captures exactly the form of spatial structure that the CAR component attempts to approximate, but in a more flexible and empirically realistic way.

(ii) *The unstructured component dominates..* With $\phi \approx 0$, residual spatial variation is essentially unstructured. This suggests that dengue in Recife does not spread primarily via geometric contiguity, but via *functional connectivity*—the way neighborhoods are linked through the road network and human mobility.

Why does the CAR component vanish? A structural interpretation

Neighborhood matrices such as Queen and Rook assume that all adjacent regions exert the *same type and intensity* of interaction, imposing a rigid homogeneous structure on space. Urban road networks, however, are highly heterogeneous: some neighborhoods are linked by multiple redundant and highly navigable paths, whereas others are connected only through narrow, long, or structurally fragile routes. This heterogeneity is not captured by traditional adjacency schemes.

Communicability curvature addresses this limitation. According to complex-network communicability theory [15], vertices with high communicability—or, in our framework, with negative correlation-weighted curvature—act as *structural emitters*: nodes that diffuse influence through multiple routes, incorporating not only

immediate neighbors but the functional connectivity of the entire network.

Thus, when curvature is included in the model:

- most of the spatial dependence that would be captured by CAR is instead absorbed by functional connectivity;
- the CAR component becomes redundant, as the latent spatial structure is already encoded in curvature;
- the residual spatial process collapses to an unstructured component, since the relevant heterogeneity has already been modeled.

This result is consistent with the literature on complex networks: communicability-based measures capture diffusion paths and higher-order connectivity patterns that neighborhood-based CAR models cannot represent, naturally replacing their role in highly heterogeneous urban systems.

Model Fit

The model exhibits strong overall fit:

$$\text{DIC} = 12928.47, \quad \text{WAIC} = 12933.86,$$

values consistent with a model in which predictors capture a substantial portion of spatial heterogeneity.

Interpretive Synthesis

The INLA/BYM2 model provides robust Bayesian evidence that:

- curvature is a structural predictor of dengue risk, with effect sizes larger than all other fixed effects;
- residual spatial dependence associated with geographic adjacency (CAR) practically disappears once functional connectivity is modeled;
- climatic, demographic, and socioeconomic covariates retain coherent directions and magnitudes;
- model stability and adequacy are excellent.

These results indicate that the geometry of the urban network—not mere geographic proximity—structures dengue diffusion in Recife [26, 27].

Building on this foundation, we extend the modeling framework to SPDE, enabling **continuous risk surfaces**, spatiotemporal interpolation, and fine-grained uncertainty quantification, with direct applications to epidemiological surveillance and territorial planning.

5. Discussion

The results of this study reveal a consistent and conceptually coherent pattern: the structure of the road network—as captured by mean communicability curvature—constitutes a robust spatial determinant of dengue incidence in the Metropolitan Region of Recife. This finding carries both theoretical and practical implications.

First, the different models estimated (Negative Binomial, fixed effects, SAR/SAC, and INLA/BYM2) converge toward the same central conclusion: curvature exhibits the most stable coefficient, with the largest magnitude and the lowest uncertainty among all covariates. This stability suggests that curvature does not merely act as a proxy for socioeconomic or climatic factors, but instead represents a structural measure of the geometry of the urban environment, conferring to it a distinct interpretative role.

From a network-theoretic perspective, more negative curvature values indicate vertices or clusters of vertices with greater capacity to “emit” influence toward adjacent regions via multiple redundant paths. These nodes function as structural dispersers, aligning with the epidemiological interpretation of neighborhoods that act as persistent hubs of dengue diffusion. As shown by Estrada and Hatano (2008), communicability synthesizes both short and long paths, a property especially relevant in dense urban settings where functional connectivity surpasses mere geographic contiguity.

This point is crucial for understanding the disappearance of the CAR term in the BYM2 model. Traditional spatial autocorrelation assumes that adjacent areas exert similar and homogeneous influence on each other. However, our results demonstrate that this assumption does not hold for Recife: the relevant spatial structure is not anchored solely in immediate adjacency but embedded within the multiple routes and interconnections of the urban fabric. By capturing this functional connectivity, curvature absorbs most of the spatial dependence that classical models would attribute to the CAR effect. The estimate $\phi \approx 0$ confirms this interpretation, indicating that nearly all structured spatial variability is explained by the covariates—particularly curvature.

From an epidemiological perspective, this implies that the spatial dynamics of dengue do not behave as a traditional local diffusion process, but rather as a phenomenon shaped by urban circulation pathways, connection density, and mobility patterns. This interpretation is consistent with recent evidence showing that human flows, urban connectivity, and micro-scale spatial accessibility play central roles in the spread of ar-

boviruses in Latin American metropolitan areas.

Finally, the results have practical implications for public-health surveillance. Variables such as precipitation, seasonality, and inequality retain coherent effects, but the inclusion of structural metrics of urban connectivity opens new possibilities for territorial monitoring: identifying structurally emissive neighborhoods, prioritizing critical intersections of the road network, and anticipating probable routes of spatial diffusion. By integrating network theory, hierarchical Bayesian modeling, and epidemiological data, this study demonstrates that continuous risk surfaces and spatiotemporal forecasts can be substantially improved by metrics that capture the functional geometry of the city.

Thus, the proposed approach offers not only statistical gains but also a conceptual perspective that complements and deepens traditional spatial models, paving the way for applications in urban planning, sanitary engineering, and public-policy strategies for combating arboviral diseases.

6. Conclusion

This study demonstrated that the mean communicability curvature of the urban road network is a structural determinant of dengue incidence in the Metropolitan Region of Recife. Through an integrated methodological strategy—combining count models, fixed effects, classical spatial specifications (SAR/SAC), and hierarchical Bayesian modeling (INLA/BYM2)—we showed that the functional geometry of the city plays a central role in shaping epidemiological risk.

The main contribution of this work lies in the consistent evidence that the connectivity of the urban network, measured through communicability curvature, captures aspects of spatial diffusion that are not accounted for by traditional models based on geographic contiguity. The practical disappearance of the structured component in the BYM2 model ($\phi \approx 0$) after introducing curvature reinforces this interpretation: the relevant spatial dependence does not arise from immediate neighborhood effects, but from multiple potential paths, road redundancies, and topological heterogeneities across the city. This confirms that urban dengue diffusion is driven more by functional connectivity than by simple physical proximity.

Environmental and socioeconomic effects—precipitation, seasonality, population density, and inequality—remained coherent across all models, reinforcing the epidemiological plausibility of the results. However, it was the inclusion of curvature that provided the largest explanatory gain, suggesting that

network-based metrics should occupy a central position in spatial analyses of arboviral diseases in complex urban environments.

From an applied perspective, the findings provide a solid foundation for the development of more precise public-health surveillance tools. By incorporating the structure of the road network into the modeling process, it becomes possible to identify structurally emissive neighborhoods, detect diffusion corridors, and enhance risk mapping to support targeted prevention and control strategies.

Finally, the results open a clear path for future research. SPDE models can extend this approach to the continuous spatial domain, enabling the construction of high-resolution risk surfaces and spatiotemporal predictions. Likewise, integrating curvature with human mobility and intra-urban transmission cycles promises significant advances in understanding arboviral dynamics in Brazilian cities.

Taken together, this study shows that incorporating structural metrics of the urban network not only improves statistical model performance but also deepens our understanding of the epidemiological process, offering an innovative perspective for spatial analyses of vector-borne diseases in urban contexts.

7. Data and Code Availability

The geocoded dengue dataset used in this study is publicly available on Zenodo [22].

All scripts used for data cleaning, graph construction, communicability curvature computation, spatial modeling (Negative Binomial, SAR/SAC, and INLA/BYM2), and figure generation are available in an open GitHub repository [23].

References

- [1] Barcellos, C.; Sabroza, P. C., *Socio-environmental determinants of dengue epidemics*, Cadernos de Saúde Pública, 17, 77–86, 2001.
- [2] Teixeira, M. G.; Costa, M. C. N.; Barreto, F.; Mota, E., *Dengue: twenty-five years since its reemergence in Brazil*, Cadernos de Saúde Pública, 25(Suppl 1), S7–S18, 2009.
- [3] Honório, N. A.; Nogueira, R. M. R.; Codeço, C. T.; Carvalho, M. S.; Cruz, O. G.; Magalhães, M. A. F. M.; Lourenço-de-Oliveira, R., *Spatial evaluation and modeling of dengue seroprevalence and vector density in Rio de Janeiro*, PLoS Neglected Tropical Diseases, 3(11), e545, 2009.

- [4] Keeling, M. J.; Rohani, P., *Modeling Infectious Diseases in Humans and Animals*, Princeton University Press, 2008.
- [5] Carvalho, M. S.; Souza-Santos, R.; Barcellos, C., *Machine learning and spatial epidemiology: A new approach to understand urban arboviruses*, Revista de Saúde Pública, 55:44, 2021.
- [6] Parselia, E.; Kontoes, C.; Tsouni, A.; Hadjichristodoulou, C.; Kioutsioukis, I.; Magiorkinis, G.; Stilianakis, N. I., *Satellite earth observation data in epidemiological modeling of malaria, dengue and West Nile virus: A scoping review*, Remote Sensing, 11(16):1862, 2019.
- [7] E. Estrada, N. Hatano, and M. Benzi. The physics of communicability in complex networks. *Physics Reports*, 514(3):89–119, 2012. doi:10.1016/j.physrep.2012.01.006.
- [8] Massaro, E.; Kondor, D.; Ratti, C., *Assessing the interplay between human mobility and mosquito-borne diseases in urban environments*, Scientific Reports, 9(1):16911, 2019.
- [9] Simoy, M. I.; Simoy, M. V.; Canziani, G. A., *The effect of temperature on the population dynamics of Aedes aegypti*, Ecological Modelling, 314:100–110, 2015.
- [10] Zheng, L.; Ren, H.-Y.; Shi, R.-H.; Lu, L., *Spatiotemporal characteristics and primary influencing factors of typical dengue fever epidemics in China*, Infectious Diseases of Poverty, 8, 1–12, 2019.
- [11] MOORE, Thomas C.; BROWN, Heidi E. Estimating *Aedes aegypti* (Diptera: Culicidae) flight distance: meta-data analysis. *Journal of Medical Entomology*, v. 59, n. 4, p. 1164–1170, 2022.
- [12] PRUSZYNSKI, Catherine A.; et al. Estimation of population age structure, daily survival rates, and potential to support dengue virus transmission for Florida Keys *Aedes aegypti* via transcriptional profiling. *PLoS Neglected Tropical Diseases*, v. 18, n. 8, p. e0012350, 2024. DOI: 10.1371/journal.pntd.0012350.
- [13] Anselin, L., *Local Indicators of Spatial Association—LISA*, Geographical Analysis, 27(2), 93–115, 1995.
- [14] DE SOUZA, Danillo Barros; DA CUNHA, Jonatas T. S.; DOS SANTOS, Everlon Figueirôa; CORREIA, Jailson B.; DA SILVA, Hernande P.; DE LIMA FILHO, José Luiz; ALBUQUERQUE, Jones; SANTOS, Fernando A. N. Using discrete Ricci curvatures to infer COVID-19 epidemic network fragility and systemic risk. *Journal of Statistical Mechanics: Theory and Experiment*, v. 2021, n. 5, p. 053501, 2021.
- [15] E. Estrada. *The Structure of Complex Networks: Theory and Applications*. American Chemical Society, 2012.
- [16] ESTRADA, Ernesto. Forman–Ricci communicability curvature of graphs and networks. *European Journal of Applied Mathematics*, p. 1–25, 2025.
- [17] GRASS-BOADA, Darian H.; DE LA NUEZ, Rodrigo; ESTRADA, Ernesto. Graph/Network Reduction Based on Communicability Vertex Similarity. 2025. (Artigo em processo de publicação; detalhes de periódico, volume e páginas ainda não disponíveis.)
- [18] Elhorst, J. P., *Spatial Econometrics: From Cross-Sectional Data to Spatial Panels*, Springer, 2014.
- [19] BLANGIARDO, M.; CAMELETTI, M. *Spatial and Spatio-Temporal Bayesian Models with R-INLA*. Chichester: Wiley, 2015.
- [20] FERREIRA DOS SANTOS, Marcílio; DOS SANTOS RODRIGUES DE MELO, Andreza. *Hierarchical Bayesian Modeling of Dengue in Recife, Brazil (2015–2024): The Role of Spatial Granularity and Data Quality for Epidemiological Risk Mapping*. arXiv e-prints, p. arXiv:2510.13672, 2025. (Preprint disponível; detalhes de periódico, volume e páginas ainda não disponíveis.)
- [21] Ferreira dos Santos, M., and Dos Santos Rodrigues de Melo, A. (2025). *Spatial and Socioenvironmental Dengue Dataset of the Recife Metropolitan Area (2015–2024)* [Data set]. Zenodo. <https://doi.org/10.5281/zenodo.17364863>.
- [22] Ferreira dos Santos, M., Dos Santos Rodrigues de Melo, A., 2025. *Dengue Cases in Recife, Brazil (2015–2024): Clean and Geocoded Dataset (v1.0)* [Data set]. Zenodo. <https://doi.org/10.5281/zenodo.17849496>.

- [23] Ferreira dos Santos, M., 2025. *Dengue Risk Modeling and Network Curvature Analysis – Code Repository*. GitHub. Available at: https://github.com/DocDengueResearcher/dengue-risk-recife-anonymous/blob/main/Graph_Prototype_2_0.ipynb.
- [24] Chinazzi, M.; Davis, J. T.; Ajelli, M.; et al., *The effect of travel restrictions on the spread of the 2019 novel coronavirus (COVID-19) outbreak*, *Science*, 368(6489), 395–400, 2020.
- [25] Adeola, A. M.; Botai, J. O.; Olwoch, J. M.; Rautenbach, C. J. H.; Adisa, O. M., *Landsat satellite-derived environmental metric for mapping mosquito breeding habitats in South Africa*, *South African Geographical Journal*, 99(1):14–28, 2017.
- [26] Borges, I. V. G.; Musah, A.; Dutra, L. M. M.; et al., *Analysis of the interrelationship between precipitation and confirmed dengue cases in the city of Recife (Brazil)*, *Frontiers in Public Health*, 12:1456043, 2024.
- [27] Oliveira, M. M.; et al., *Dengue Monitoring Dashboard: A tool to support public health management in Brazil*, *Cadernos de Saúde Pública*, 38:e00252021, 2022.
- [28] Anselin, L., *Spatial Econometrics: Methods and Models*, Kluwer Academic Publishers, Dordrecht, 1988.
- [29] LeSage, J. P.; Pace, R. K., *Introduction to Spatial Econometrics*, CRC Press, 2009.
- [30] Florax, R. J.; Folmer, H.; Rey, S. J., *Specification searches in spatial econometrics: The relevance of Hendry's methodology*, *Regional Science and Urban Economics*, 33(5), 557–579, 2003.
- [31] Rue, H.; Martino, S.; Chopin, N., *Approximate Bayesian inference for latent Gaussian models by using integrated nested Laplace approximations*, *Journal of the Royal Statistical Society: Series B*, 71(2), 319–392, 2009.
- [32] Riebler, A.; Sørbye, S. H.; Simpson, D.; Rue, H., *An intuitive Bayesian spatial model for disease mapping that accounts for scaling*, *Statistical Methods in Medical Research*, 25(4), 1145–1165, 2016.
- [33] Lindgren, F.; Rue, H.; Lindström, J., *An explicit link between Gaussian fields and Gaussian Markov random fields: the SPDE approach*, *Journal of the Royal Statistical Society: Series B*, 73(4), 423–498, 2011.